

氧燃烧方式下煤粉锅炉辐射传热特性分析

王小华¹, 刘 豪¹, 邱建荣¹, 盛昌栋²

(1 华中科技大学 煤燃烧国家重点实验室, 湖北 武汉 430074; 2 东南大学 能源与环境学院, 江苏 南京 210096)

摘 要: 氧燃烧方式是一种能综合控制燃煤污染物排放的新型洁净燃烧技术, 有关该方式下煤粉锅炉传热特性的研究对于老机组改造及新机组的重建具有非常重要的意义。以某电厂 300 MW 燃煤锅炉为例, 针对氧燃烧方式下燃烧介质的物理特性发生变化, 通过引入循环率的概念, 提出并发现了氧燃烧方式下必须考虑 CO₂、H₂O、O₂、H₂ 的 5 种高温分解反应, 在此基础上修正并发展了新的适用于氧燃烧方式下绝热火焰温度、锅炉辐射传热的计算方法。结果表明, 修正后的辐射传热计算公式在氧燃烧方式下具有良好的通用性, 在干、湿两种烟气循环方式下, 绝热火焰温度随循环率的增加非线性降低; 当干烟气、湿烟气的循环率分别在 0.71 和 0.67 附近时, 获得与常规燃烧方式相同的烟气平均温度和辐射传热量。

关 键 词: 燃煤锅炉; 氧燃烧; 绝热火焰温度; 辐射传热; 传热特性; 循环率

中图分类号: TQ534 文献标识码: A

引 言

燃煤 CO₂ 的排放导致全球气候变暖已成为国际社会关注的一个焦点。氧燃烧方式是一种能够综合控制燃煤污染物排放的新型洁净燃烧技术。它是将 O₂ 与循环烟气混合代替空气作为介质参与燃烧, 烟气中 CO₂ 浓度升高使得 CO₂ 回收成本降低, 而且还能够同时减少 SO_x、NO_x 的排放^[1]。

与常规燃烧方式相比, 由于气体产物的辐射性质和气体热容量发生了变化, 导致氧燃烧方式下燃煤锅炉的传热特性有较大不同。国内外学者对氧燃烧方式下煤的燃烧特性开展了大量的实验研究^[2-5], 但是在利用常规燃烧方式下的辐射传热计算公式进行氧燃烧方式下辐射传热计算所开展的工作尚不多见。本文以某电厂 300 MW 燃煤锅炉为例, 在常规燃烧方式下计算辐射传热的基础上, 进行公式修正, 修正后的公式可用于对锅炉氧燃烧方式改造的辐射传热计算。

1 计算过程及方法

1.1 计算条件

计算所选电厂的锅炉炉膛参数和煤质分析如表 1 和表 2 所示。

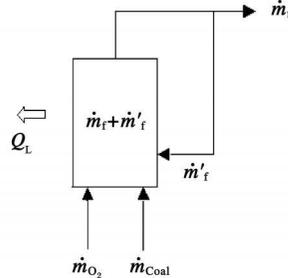
表 1 锅炉炉膛参数

额定蒸发量 / t·h ⁻¹	给煤量 / t·h ⁻¹	炉膛容积 / m ³	炉膛表面积 / m ²	一次风温 / °C	一次风率 / %
1 000	150	7 000	2 123.6	370	18

表 2 煤质分析

C _{ar} / %	H _{ar} / %	O _{ar} / %	N _{ar} / %	S _{ar} / %	A _{ar} / %	M _{ar} / %	低位发热量 / kJ·kg ⁻¹
56.44	2.79	3.30	0.54	0.47	26.76	9.70	21 744

在氧燃烧方式下, 循环率定义为循环率等于循环的烟气质量流量与总质量流量的比值^[3], 如图 1 所示。



其值计算表达式为:

$$R_{\text{recycle}} = \frac{m'_f}{m'_f + m_f} \quad (1)$$

式中: m'_f —循环的烟气质量流量, kg/s; m_f —排放的烟气质量流量, kg/s。在计算过程中, 为方便计算, 在不影响结果的前提下, 做出如下假设:

图 1 氧燃烧方式循环示意图

- (1) 各种情况下, 送入炉膛的气体温度与空气气氛下相同, 即风粉混合温度 515 K;
- (2) 煤粉完全燃烧;
- (3) 循环烟气: 干烟气为 CO₂ 和 O₂, 湿烟气为 CO₂、H₂O 和 O₂;
- (4) 煤粉燃烧产生的 NO_x、N₂ 忽略不计, SO₂ 计入 CO₂ 中;

收稿日期: 2008-04-01; 修订日期: 2008-11-28

基金项目: 国家重点基础研究专项经费基金资助项目(2006CB705807); 国家杰出青年基金资助项目(50525619); 教育部科学研究重大基金资助项目(306012)

作者简介: 王小华(1982), 男, 湖北仙桃人, 华中科技大学硕士研究生。http://www.cnki.net

(5) 烟气中的氧气浓度控制与常规燃烧方式相同, 为 3.3(V%);

(6) 不考虑炉膛漏风的影响。

1.2 常规燃烧方式下辐射传热计算

火焰与炉壁之间的换热可简化成为两个互相平行的无限大平面间的辐射换热^[6]。炉膛传热基本方程为:

$$A_b \Psi a_1 \sigma_0 T_{hy}^4 = \varphi B_j V C_{pj} (T_{11} - T''_1) \quad (2)$$

式中: σ_0 —绝对黑体辐射常数, 其值: 5.67×10^{-11} kW/(m²·K⁴); A_b —炉壁面积, m²; Ψ —热有效系数, 可通过试验确定; T_{hy} —火焰的平均温度, K; φ —保热系数; B_j —计算燃料消耗量, kg/h; $V C_{pj}$ —烟气的平均比热容, kJ/(kg·K); T_{11} —绝热火焰温度, 亦称绝热燃烧温度, K; T''_1 —炉膛出口温度, K; a_1 —炉膛黑度, 其计算式为:

$$a_1 = \frac{a_{hy}}{a_{hy} + (1 - a_{hy}) \Psi} \quad (3)$$

式中: a_{hy} —火焰黑度。

式(2)两边同时除以 T_{11}^4 , 并令:

$$Bo = \frac{\varphi B_j V C_{pj}}{\sigma_0 \Psi A_b T_{11}^3} \quad (4)$$

可以得到:

$$\Theta_1^{4n} = \frac{Bo}{a_1} (1 - \Theta_1) \quad (5)$$

式中: $\Theta = T/T_{11}$ —无因次温度, 表示火焰温度与绝热火焰的比值。通过大量试验研究, 经整理得出半经验计算式^[6]:

$$\Theta_1'' = \left(\frac{Bo}{a_1}\right)^{0.6} / [M + \left(\frac{Bo}{a_1}\right)^{0.6}] \quad (6)$$

最后得到炉膛出口烟温的表达式:

$$\theta_1'' = \frac{T_{11}}{M(a_1/Bo)^{0.6} + 1} - 273 \quad (7)$$

式中: M —考虑燃烧条件影响的参数。

1.3 常规燃烧方式下辐射传热计算的修正

氧燃烧方式下, 由于烟气中 CO₂ 浓度发生了变化, 在计算火焰黑度时必须考虑由 H₂O 和 CO₂ 光带部分重叠而引入的修正量^[7~8]; 此外, 常规燃烧方式下由于绝热火焰温度较低; 即使考虑分解时, 主要的烟气产物 CO₂、H₂O 的分解率较低, 因此可以忽略不计; 而氧燃烧方式下, 循环率较低时, 燃烧温度高, 气体产物的分解率高, 必须考虑气体产物的分解。

1.3.1 火焰黑度计算修正方法

火焰黑度的计算式为^[6]:

$$a_{hy} = 1 - e^{-kp\delta} \quad (8)$$

式中: P —炉膛压力, 对一般锅炉取 0.1 MPa; k —火

焰辐射减弱系数, (m³MPa)⁻¹, 可认为是各辐射成份减弱系数的代数和:

$$k = (k_q - \Delta k)r + k_h \mu_h + k_j x_1 x_2 \quad (9)$$

式中: k_q —三原子气体的辐射减弱系数, (m³MPa)⁻¹; r —三原子气体总容积分数; k_h —火焰中悬浮灰粒的辐射减弱系数, (m³MPa)⁻¹; μ_h —飞灰浓度, kg/kg; k_j —火焰中焦炭颗粒的辐射减弱系数, 取 10(m³MPa)⁻¹; x_1 、 x_2 —煤种、燃烧方式对焦炭浓度的影响系数。

对气体辐射减弱系数的修正方法采用 Lechner 提出的宽带模型修正式^[10]:

$$\Delta k = \left\{ \frac{\zeta}{10.7 + 101 \cdot \zeta} - 0.089 \zeta^{10.4} \right\} \lambda^{2.76} \quad (10)$$

$$\zeta = \frac{P_{H_2O}}{P_{H_2O} + P_{CO_2}} \quad (11)$$

$$\lambda = \log((P_{H_2O} + P_{CO_2}) \delta) \quad (12)$$

式中: P_{H_2O} —水蒸气的分压, MPa; P_{CO_2} —二氧化碳的分压, MPa; δ —有效辐射层厚度, cm; 对炉膛来说, 可表示为:

$$\delta = 3.6 \frac{V_1}{A_b} \quad (13)$$

式中: V_1 —炉膛容积, m³。

1.3.2 绝热火焰温度计算的修正方法

氧燃烧方式下绝热火焰温度的计算, 主要是考虑高温下气体分解的影响^[9]。即 $Q_{LJ} \neq 0$; 计算绝热火焰温度的表达式为:

$$T_{11} = \frac{Q_{dw} + I_{rk} - Q_{LJ}}{(1 + \alpha L^0) \cdot C_{yq}} \quad (14)$$

式中: Q_{dw} —燃料的低位发热量, kJ/kg; I_{rk} —燃料及供给燃烧用空气在供给温度时的热焓, 即显热, kJ/kg; Q_{LJ} —燃烧产物由于离解而吸收的热量, kJ/kg; T_{11} —烟气的温度, 即燃料的燃烧温度, °C; C_{yq} —烟气的比热, 取决于烟气的组成, kJ/(kg·°C); $1 + \alpha L^0$ —烟气的质量, kg; 当完全燃烧时 $\alpha = 1$ 。

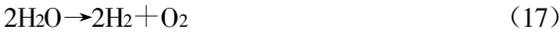
常规绝热火焰温度的计算中, 气体产物分解率的数据目前还不完整, 因此采用 F * A * C * T 软件包完成热力学平衡计算, 它是一种基于系统总吉布斯自由能最小化原理的热力学计算程序^[10], 由于其整合了大量纯物相的热力学特性数据库, 这使得在计算平衡产物时较为有利。热力学平衡计算以煤作为计算的初始成份, 为简化计算, 仅考虑 C、H、O、N、S 等物质的反应。计算以 1 kg 煤为基准, 理论氧气量按 $V^0 = 0.01866[C] + 0.007[S] + 0.055[H] - 0.007[O]$ 得到, 氧气过量系数为实际氧气量与理论氧气量的比, 由循环率而定。初始条件如下: 压力:

$1.01 \times 10^5 \text{ Pa}$; 温度: 风粉混合温度, 515 K.

2 计算结果及分析

2.1 气体产物分解对绝热火焰温度的影响

根据计算得到的产物组分及浓度结果, 并参考高温下气体分解反应^[9], 发现在高温下气体产物分解主要是 5 个化学反应:



在考虑上述气体产物分解后, 计算得到的不同循环率下绝热火焰温度的变化曲线, 并与不考虑气体产物分解时的计算结果作比较, 如图 2 所示。

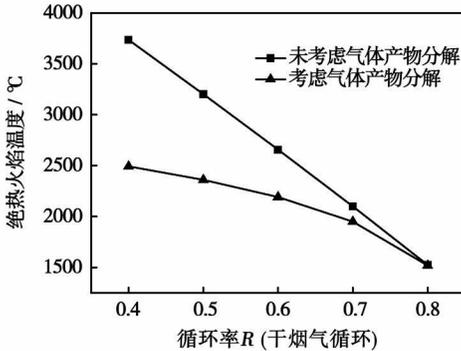


图 2 考虑气体产物分解前后绝热火焰温度的比较

从图 2 可以看出: 在干循环方式下, 随着循环率的增加, 绝热火焰温度存在递减的趋势, Zheng Changhao 等人认为^[5]: 在低循环率下, 氧气浓度随之升高, 从而可能导致燃烧速率、燃烧效率升高; 同时气体产物的烟气质量流量降低, 从而使绝热火焰温度升高。Khare S P 等人通过对绝热火焰温度的研究认为^[4]: 绝热火焰温度随着氧气浓度的增加呈线性关系变化。图中所示的趋势与 Zheng Changhao 等人的计算结果较为吻合。且二者之间的温差呈增大的趋势, 这是因为在不同的绝热火焰温度下气体的分解存在差异: 在高温条件下, 分解反应为吸热反应, 根据吕·查德里反抗规则, 平衡向吸热的方向移动以抑制温度升高的影响, 分解率会增加^[9]。绝热火焰温度随循环率的变化不是一个单值函数, 需要综合考虑氧气、二氧化碳浓度和烟气比热容的影响。

考虑式(15)~式(19)这 5 个分解反应, 应用常规计算方法计算的结果与 F * A * C * T 软件包 Equilib 模块计算的结果的对比如图 3 所示。从图 2

可以看出: 在两种方法下, 得到的结果是吻合的。说明在循环中只考虑上述 5 个分解反应是认可的。

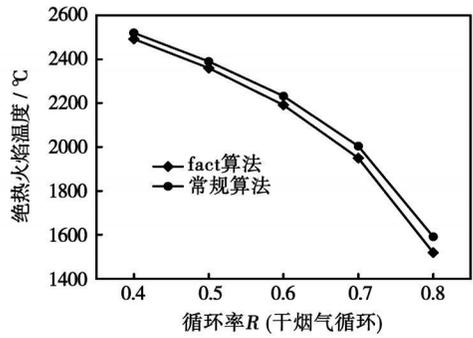


图 3 不同计算方法的绝热火焰温度的对比

2.2 不同循环方式下绝热火焰温度、炉膛出口温度、传热量的计算结果分析

图 4 为不同循环率下绝热火焰温度的计算结果。图中表明, 随着循环率的增加, 绝热火焰温度逐渐降低。因为循环率增加时, 氧气浓度降低, 可能导致燃烧速率、燃尽率的降低; 同时烟气量增加, 烟气比热容亦增大, 绝热火焰温度降低。

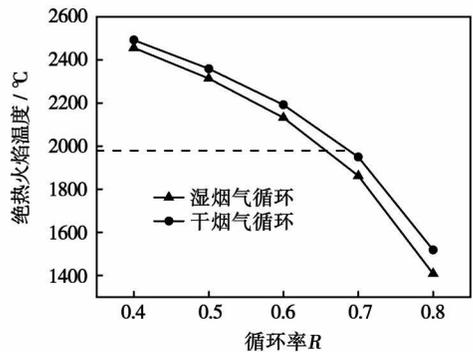


图 4 不同循环率下的绝热火焰温度计算结果

图 5 为炉膛出口温度变化曲线。图中表明, 随着循环率增加, 炉膛出口温度亦逐渐降低。以 T_{11} 为变量, 式(7)对 T_{11} 求导数, 得到表达式:

$$\frac{\partial \theta''_1}{\partial T_{11}} = \frac{1 - 0.8AT_{11}^{1.8}}{(1 + AT_{11}^{1.8})^2} \quad (20)$$

式中: A —变化不大的量, 可表示为:

$$A = M \left(\frac{\sigma_0 \Psi_{Abal}}{Q_{Bj} V_{Cpj}} \right)^{0.6} \quad (21)$$

从式(20)可以看出: 当 $1 - 0.8AT_{11}^{1.8} < 0$, 即绝热火焰温度很大时, 炉膛出口温度随绝热火焰的增加而减少; 而 $1 - 0.8AT_{11}^{1.8} > 0$, 即绝热火焰温度小时, 炉膛出口温度随绝热火焰的增加而增加; 在计算中 T_{11} 是一个较小的量, $1 - 0.8AT_{11}^{1.8} > 0$, 则炉膛出口温度随绝热火焰的降低而降低。

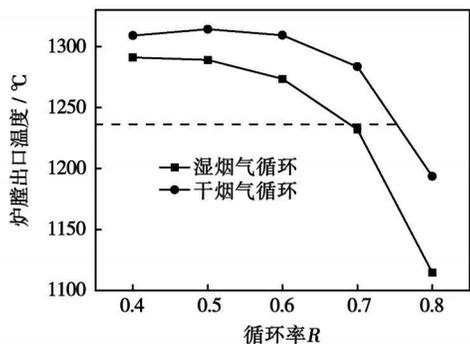


图 5 不同循环率下炉膛出口温度的计算结果

图 6 为烟气平均温度变化曲线。图中表明：随着循环率的增大，气流温度是逐渐降低的。气流平均温度计算式为^[11]：

$$T = 0.925 \sqrt{T_{11} \cdot T'_{11}} - 273 \quad (22)$$

绝热火焰温度、炉膛出口温度随循环率的增大而降低，则气流平均温度也是降低的。

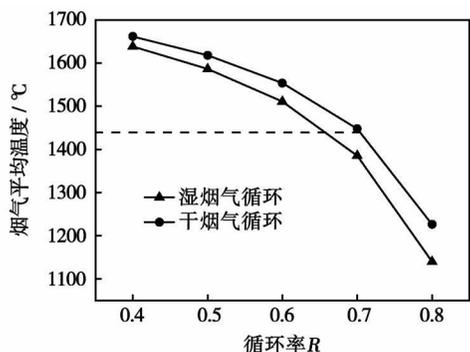


图 6 不同循环率下烟气平均温度的计算结果

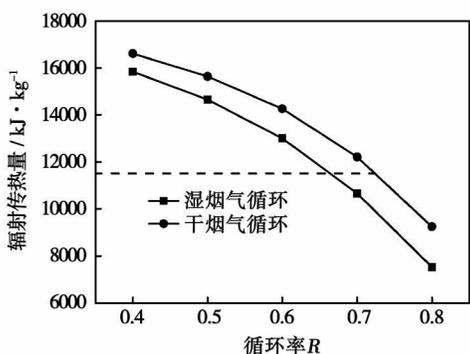


图 7 不同循环率下炉膛辐射传热量的计算结果

图 7 为传热量的变化曲线。图中表明，随着循环率的增大，传热量是逐渐降低的。因为随着循环率的增加，炉膛绝热火焰温度是降低的，而烟气平均比热容的升高比绝热火焰温度的降低慢，炉膛传热量随循环率的增加而降低。要达到与空气气氛下相同的辐射传热性能，干、湿烟气循环率分别为 0.71、0.67，此时入口处氧气的浓度为：干烟气：29.2%，湿

烟气：28.4%；这一结论与 Thambijuthu Kelly V 和 Wang C S 等人实验结论是一致的^[2~3]。仅从烟气平均温度和辐射传热的角度看，干烟气循环和湿烟气循环对氧燃烧方式都是合适的，但综合锅炉结渣、腐蚀和磨损等因素的影响，以干烟气循环为佳。

3 结 论

(1) 氧燃烧方式下，绝热火焰温度的计算时，需要考虑高温下气体产物的分解，结合 F * A * C * T 软件包对其燃烧产物分析，发现了气体产物中需要考虑的 5 个主要分解反应，在考虑气体分解后，绝热火焰温度随循环率的增加呈非线性变化；

(2) 烟气循环时，干烟气、湿烟气的循环率分别为 0.71、0.67 时，获得与常规燃烧方式相同的辐射传热性能；

(3) 仅从烟气平均温度和辐射传热的角度看，干烟气循环和湿烟气循环对氧燃烧方式都是合适的，但综合锅炉结渣、腐蚀、磨损等因素的影响，以干烟气循环为佳。

参考文献：

- [1] 骆仲尧, 毛玉如, 吴学成. O₂/CO₂ 气氛下煤燃烧特性试验研究与分析 [J]. 热力发电, 2004, 33 (06): 14—18
- [2] TAN YEWEN, CROISSET ERIC, DOUGLAS MARK A, et al. Combustion characteristics of coal in a mixture of oxygen and recycled flue gas [J]. Fuel, 2006, 85 (4): 507—512
- [3] WNAG C S, BERRY G F, CHANG K C, et al. Combustion of pulverized coal using waste carbon dioxide and oxygen [J]. Combustion and Flame, 1988, 72 (3): 301—310
- [4] KHARE S P, WALL T F, GUPTA R P. Retrofitting of air-fired pf plant to oxy-fuel; combustibility and heat transfer impacts // The 30th International Technical Conference on Coal Utilization and Fuel System [C]. Clearwater; U. S. Department of Energy and Coal Technology Association, 2005, 651—663
- [5] ZHENG CHANGHAO, CLEMENTS BRUCE, ZHENG LIGANG. The feasibility of decreased furnace size with reduced flue gas re-circulation in coal-fired boiler designs // The 30th International Technical Conference on Coal Utilization and Fuel System [C]. Clearwater; U. S. Department of Energy and Coal Technology Association, 2005, 561—575
- [6] 陈学俊, 陈听宽. 锅炉原理 [M]. (第二版). 北京: 机械工业出版社, 1991
- [7] 杨世铭, 陶文铨. 传热学 [M]. (第三版). 北京: 高等教育出版社, 1998
- [8] LECKNER B. Spectral and total emissivity of water vapor and carbon dioxide [J]. Combustion & Flame, 1972, 19 (1): 33—48.
- [9] 张松寿. 工程燃烧学 [M]. 上海: 上海交通大学出版社, 1987.
- [10] BALE C W, PELTON A D, THOMPSON W T. F * A * C * T 2. 1-user manual [EB]. <http://www.crct.polymtl.ca>, 1996
- [11] 陈春元. 大型煤粉锅炉燃烧设备性能设计方法 [M]. 哈尔滨: 哈尔滨工业大学出版社, 2002.

(编辑 滨)

jing, China, Post Code: 100011), HUANG Xiang, XU Yan-qiang (China Huadian Engineering (Group) Co. Ltd., Beijing, China, Post Code: 100044)// Journal of Engineering for Thermal Energy & Power. - 2009,24(1). - 73 ~ 76

A direct air-cooled condenser consists of several direct air-cooled elements. A study of its elements is of major importance. Based on a practical engineering project, the flow and heat transfer performance of a 135 MW direct air-cooled condenser sample unit has been studied. By using a numerical heat transfer (NHT) software Fluent, a numerical simulation has been performed of the air-cooled sample unit at its design and test operating conditions. The reason why the simulation results differ from the design and test data was analyzed. The simulation, analysis and study of the external air speed and temperature field of the direct air-cooled condenser can be helpful for the optimized design of the systems in question. **Key words:** direct air-cooled condenser, sample unit, numerical simulation, optimized design

常规工况下多弯头数脉动热管运行性能的实验研究 = **Experimental Study of the Operation Performance of Multi-elbow Pulsating Heat Pipes at Conventional Operating Conditions** [刊, 汉] / YANG Hong-hai, WAN Qing, HAN Hong-da (College of Environment Science and Engineering, Donghua University, Shanghai, China, 201620) // Journal of Engineering for Thermal Energy & Power. - 2009,24(1). - 77 ~ 80

Two groups of pulsating heat pipes consisting of 40 thin copper tube elbows with an inner diameter of 1 and 2 mm respectively were designed. Two loop types, closed or open, can be made available by opening or closing a valve in the pipe. With R123, water and alcohol serving as working media respectively, liquid filling rate ranges from 15% to 95% and the installation angle can be regulated freely. Through tests, analyzed and compared was the influence of the inner diameter, working medium, liquid filling rate, heating angle and loop type of the multi-elbow pulsating heat pipe on its startup and heat transfer performance at conventional operating conditions. **Key words:** pulsating heat pipe, number of elbows, loop type, operation performance, influencing factor

超临界变压运行直流锅炉中间集箱分配特性的试验研究 = **Experimental Study of Intermediate Header Flow Distribution Characteristics of a Supercritical Once-through Boiler Operating at Variable Pressures** [刊, 汉] / ZHU Yu-qin (Technology Research Center of Petroleum Refinery Engineering, Xi'an Shiyou University, Xi'an, China, Post Code: 710065), BI Qin-cheng, CHEN Ting-kuan (National Key Laboratory on Multi-phase Flows in Power Engineering, Xi'an Jiaotong University, Xi'an, China, Post Code: 710049) // Journal of Engineering for Thermal Energy & Power. - 2009,24(1). - 81 ~ 84

In the light of the structural and parameter features of an intermediate header serving as a transition connection between the spiral coil-tube water-wall at the lower part of the furnace and the vertical tube water-wall at the upper part of the furnace in a 600 MW supercritical boiler, the distribution characteristics of gas-liquid two-phase flows in the intermediate header of the supercritical boiler at a load of 35% ECR (Economical Continuous Rating), 50% ECR and 75% ECR were simulated by using an air-water test loop. Through observations and a high-speed photographic method, the flow pattern in parallel branch tubes of a distribution header was measured and analyzed. By using a quick-closing valve and friction resistance method, measured respectively were the phase and flow distribution among various branch tubes. The test results show that at three operating conditions and with inlet dryness ranging from $x = 0.7$ to 0.95, the flow distribution of the air-water two-phase flows passing through the parallel branch tubes of the distribution header is comparatively uniform, and in most cases, the flow rate deviation is less than 10%. **Key words:** supercritical once-through boiler, header, distribution characteristics, air-water two-phase flow

氧燃烧方式下煤粉锅炉辐射传热特性分析 = **Thermodynamic Calculation of Radiative Heat Transfer in a Coal-**

fired Boiler under an Oxygen Combustion Mode[刊,汉]/ WANG Xiao-hua, LIU Hao, QIU Jian-rong (National Key Laboratory on Coal Combustion, Huazhong University of Science and Technology, Wuhan, China, Post Code: 430074), SHENG Chang-dong (College of Energy Source and Environment, Southeast University, Nanjing, China, Post Code: 210096)// Journal of Engineering for Thermal Energy & Power. - 2009, 24(1). - 85 ~ 88

Oxygen combustion mode is a new type of clean combustion technology for the comprehensive control of pollutant emissions from coal-combustion. The investigation of the heat transfer characteristics of a coal-fired boiler under the mode mentioned earlier is of the utmost importance for the reconstruction of old thermal power plants and retrofitting of new ones. With a 300 MW coal-fired boiler in a power plant serving as an example, in the light of changes occurring to the physical properties of combustion media under the new combustion mode and through an introduction of the concept of circulating rate, proposed and identified were five pyrolysis reactions of CO_2 , H_2O , O_2 and H_2 necessary to be taken into account under the combustion mode in question. On this basis, corrected and developed was a new method for calculating the adiabatic flame temperature and radiative heat transfer suitable for the combustion mode. The research results show that the corrected radiative heat transfer calculation formulae display a good universality under the oxygen combustion mode. Under the two types of dry and wet flue gas circulating mode, the adiabatic flame temperature decreases nonlinearly with an increase of the circulating rate. When the circulating rates of the dry and wet flue gases are around 0.71 and 0.67 respectively, flue-gas average temperature and radiative heat-transfer rate are obtained, which are identical to those of a conventional combustion mode. **Key words:** coal-fired boiler, oxygen combustion, adiabatic flame temperature, radiative heat transfer, heat transfer characteristics, circulating rate

O_2/CO_2 气氛快速升温煤焦低温氮吸附等温线形态分析 = Morphological Analysis of Low-temperature Nitrogen Adsorption Isothermal Curves of Coal Coke Undergoing a Quick Temperature Rise in an O_2/CO_2 Atmosphere [刊,汉]/ LI Qing-zhao, ZHAO Chang-sui, WU Wei-fang, et al (College of Energy Source and Environment, Southeast University, Nanjing, China, Post Code: 210096)// Journal of Engineering for Thermal Energy & Power. - 2009, 24(1). - 89 ~ 94

By utilizing a sedimentation furnace test device with thermodynamic operating conditions similar to those of an actual pulverized-coal boiler and under the condition of quickly rising temperatures, prepared were coal coke samples in two combustion atmospheres (O_2/CO_2 and O_2/N_2), with different oxygen concentrations and residence times. By using an AS-AP2020M type of full-automatic specific surface area and porosimeter, determined were the low-temperature nitrogen adsorption isothermal curves of various coal coke samples. The analytic results show that the shapes of adsorption isothermal curves obtained from the coal coke samples under various conditions are all typical adsorption isothermal curves of Type II (reversed S shape). The coal coke has a relatively continuous and integral pore system with pore diameters ranging from the smallest molecular grade (pore diameter about 0.86 nm) to the largest without an upper limit (relative). It can be seen from an analysis of the shapes of the adsorption loop curves that the pore of the coal coke samples may contain many blind pores (cylindrical holes and parallel plate-shaped or cut-pointed ones with one closed end) that produce no adsorption loop curves, including a portion of cracking pores. It has been found that a change of combustion atmosphere causes no marked changes in the formation and development of pores during the combustion of coal coke. However, compared with the isothermal curves obtained from the coal coke samples in the O_2/N_2 atmosphere, those obtained in the O_2/CO_2 atmosphere feature a slight difference, indicating a different pore diameter distribution of the coal coke samples in various conditions. The test results have provided a certain basis for a further investigation of the combustion process of pulverized coal in a high concentration CO_2 atmosphere and its difference from a conventional combustion mode. **Key words:** O_2/CO_2 atmosphere, quick temperature rise, pore structure, adsorption isothermal curve, adsorption loop curve